Characterization of Functionally Relevant Residues of *Escherichia coli* Multi-Drug Efflux Pump Protein AcrB

by

Mellecha Blake

A Thesis Presented in Partial Fulfillment
of the Requirements for the Degree
Master of Science

Approved July 2016 by the
Graduate Supervisory Committee:

Rajeev Misra, Chair
Xuan Wang
Valerie Stout

ARIZONA STATE UNIVERSITY

August 2016

ABSTRACT

Emergence of multidrug resistant (MDR) bacteria is a major concern to global health. One of the major MDR mechanisms bacteria employ is efflux pumps for the expulsion of drugs from the cell. In *Escherichia coli*, AcrAB-TolC proteins constitute the major chromosomally-encoded drug efflux system. AcrB, a trimeric membrane protein is well-known for its substrate promiscuity. It has the ability to efflux a broad spectrum of substrates alongside compounds such as dyes, detergent, bile salts and metabolites. Newly identified AcrB residues were shown to be functionally relevant in the drug binding and translocation pathway using a positive genetic selection strategy. These residues—Y49, V127, D153, G288, F453, and L486—were identified as the sites of suppressors of an alteration, F610A, that confers a drug hypersensitivity phenotype. Using site-directed mutagenesis (SDM) along with the real-time efflux and the classical minimum inhibitory concentration (MIC) assays, I was able to characterize the mechanism of suppression.

Three approaches were used for the characterization of these suppressors. The first approach focused on side chain specificity. The results showed that certain suppressor sites prefer a particular side chain property, such as size, to overcome the F610A defect. The second approach focused on the effects of efflux pump inhibitors. The results showed that though the suppressor residues were able to overcome the intrinsic defect of F610A, they were unable to overcome the extrinsic defect caused by the efflux pump inhibitors. This showed that the mechanism by which F610A imposes its effect on AcrB function is different than that of the efflux pump inhibitors. The final approach was to determine whether suppressors mapping in the periplasmic and trans-membrane

domains act by the same or different mechanisms. The results showed both overlapping and distinct mechanisms of suppression.

To conclude, these approaches have provided a deeper understanding of the mechanisms by which novel suppressor residues of AcrB overcome the functional defect of the drug binding domain alteration, F610A.

DEDICATION

I dedicate this work to the Almighty Father, Mother Mary and all the angels and saints whom I have prayed to for guidance and wisdom. I would like to especially acknowledge Saint Joseph of Cupertino for help with many examinations during my time here in graduate school. I thank the Newman Center for all their spiritual support. I thank my family and friends for also supporting encouraging me. I thank Kiah Singleton for being my bestie for the restie. I thank all my friends in the Hayden and Noble Library. I thank Gary Tahmahkera for saving my butt with a P2 and a refrigerator. I thank Hyun Jae Cho and Julian Yu for feeding me awesome food and being there for me when I needed advice. I thanks to all the people in the SoLS department whom have always been kind to me. I would like to especially thank Dr. Misra for making me a better person than I could ever imagine being.

TABLE OF CONTENTS

Page

LIST OF TABLES

Table Page

LIST OF FIGURES

CHAPTER 1

INTRODUCTION

Antibiotics Resistance: A Global Health Concern

The discovery of penicillin, commonly known as the "miracle drug", by Alexander Fleming in 1929, ushered in the era of antibiotics (Fleming, 1942). Within a decade after its discovery, the drug was mass-produced for the treatment of streptococcal, staphylococcal, and gonococcal infections. As the drug became widely used, the inevitability of penicillin-resistant bacteria emerged. Penicillin-resistant *Staphylococcus aureus* was identified in the mid-1940s, just a few years after the release penicillin for therapeutic use. To date *S. aureus* continues to be a global health concern as newer β-lactam drugs, such as methicillin, are no longer effective treatments (David and Daum, 2010).

The history of penicillin and penicillin-resistant *S. aureus* broadly describes the evolutionary race between antibiotics and resistant bacteria (Aminov, 2010; Alanis, 2005; Davies and Davies, 2010). The increase use of antibiotics has resulted in the emergence of resistant bacteria. And to overcome the resistant bacteria new antibiotics must be developed or discovered for treatment. Unfortunately, the development of drugs has not kept up with the spread of resistant bacteria. Also, antibiotics are extensively used, such in the livestock industry (Chuach, 2016; Aarestrup *et al.*, 2001; Bywater *et al.* 2005) and even sometimes misused by clinician, physician and dentists globally (Weinstein, 2001; Monroe and Polk, 2000; Sweeney *et al*., 2004). The inappropriate uses even extend to the patients who do not understand appropriate dosage requirements (Okeke *et al.*, 1999).

The combined issues of the lack of new antibiotics and the misuse of existing antibiotics have consequently allowed for the emergence of multi-drug resistant (MDR) bacteria such as Methicillin-Resistant *Staphylococcus aureus* (MRSA) and Carbapenem-resistant *Enterobacteriaceae* which are resistant to even the "last resort" antibiotics (Levy and Marshall, 2004; WHO 2014).

Mitigation of the emergence of drug-resistance bacteria requires a fundamental understanding of the mechanisms by which the bacteria have adapted to an environment of excessive antibiotic use. Bacteria are constantly acquiring random mutations and mobile elements, such as plasmids, via horizontal gene transfer. When a bacterial population is exposed to selective pressures (e.g. in the presence of antibiotics) the majority of bacterial cells will be killed, while some will survive. Those that survived likely contain certain genetic variations that allowed them to overcome killing by the antibiotic. Therefore, certain specific genetic variations are beneficial because they allow bacterial survival under adverse conditions. This increases the fitness and the adapted genotype will be fixed with time.

The acquisitions of resistance are evolutionary adaptations that act as a defense against antibiotics. There are four general modes of resistance bacteria utilize: (1) Alteration of the target protein to interfere with drug binding. For example, alteration in the DNA gyrase can lessen or eliminate the interaction of the clinically used fluoroquinolone antibiotics (Hooper, 1999; Mehla and Ramana, 2016). (2) Production of degradative enzymes such as β-lactamase, a periplasmic enzyme, which cleaves the β-lactam ring of the antibiotic to inactivate antibiotic like penicillin (Abraham and Chain; 1940). (3) Decrease in outer membrane (OM) permeability, such as the regulation of

porins expression to reduce influx of some antibiotics like β-lactams and chloramphenicol (Nikaido, 2003; Delcour, 2009). (4) Increase expression of antibiotic efflux pumps that actively export antibiotics into the extracellular space. MDR bacteria commonly utilize multiple mechanisms of antibiotic resistances simultaneously. Gram-negative bacteria, however, have the advantage of synergy with outer membrane permeability barrier and the antibiotic efflux pumps.

Efflux pumps have been classified into several superfamilies: ATP binding cassettes (ABC); major facilitator superfamily (MFS); multidrug and toxic-compound extrusion (MATE); small multidrug resistance (SMR); and resistance nodulation division (RND). The superfamilies differ based on energy used to export the substrates and their organization within the inner membrane or outer membrane. The ABC pumps use ATP for export while the other members use proton motive force via the proton gradient. The SMR and MFS are solitary pumps located in the cytoplasmic or inner membrane. MATE, ABC, and RND are tripartite systems, in which the inner membrane-localized efflux pump interacts with a periplasmic protein and an outer membrane protein (Li *et al*., 2015). The tripartite systems are more efficient for resistance since the substrates are exported completely out of the cell into the extracellular space. The solitary pumps export substrates into the periplasm where the antibiotic can easily re-enter the cytoplasm. Resistance can be increased by tripartite systems capturing substrates exported by solitary pumps, therefore having a synergistic relationship (Lee *et al*., 2000).

AcrAB-TolC Efflux System

The RND superfamily members are ubiquitous efflux systems of Gram-negative bacteria and are huge contributors for resistance of common antimicrobial compounds (Kumar and Schweizer, 2005). The *Enterobacteriacea* family is coincidently the largest family of Gram-negative bacteria that are multidrug resistant. AcrB, an archetypal member of the RND efflux pump family, is constitutively expressed proton-substrate antiporter and is the primary efflux pump utilized in *Escherichia coli* (Ma *et al*., 1995). AcrB, like other members of this superfamily, functions in a tripartite manner by interacting with AcrA, a periplasmic protein and TolC, which is the β-barrel outer membrane protein (Paulsen *et al.*, 1997). AcrA is a member of the membrane fusion protein (MFS) superfamily (Dinh *et al*., 1994). It is a lipoprotein and hence anchored in the inner membrane through its amino terminus, while remainder of the protein is exposed in the periplasm. TolC is a multi-functional outer membrane protein, which, besides expelling antibiotics and other AcrB substrates out of the cell, also aid in the import of colicin E1, a toxin protein produced by certain *E. coli* strains (Masi *et al*., 2007) and export of α-hemolysin (Wandersman and Delepelaire, 1990).

In the AcrAB-TolC efflux system all three proteins are essential for substrate efflux. The structure of each component has been solved (AcrA, Mikolosko *et al*., 2006; AcrB, Seeger *et al*., 2006 and Murakami *et al*., 2006; TolC, Koroakis *et al*., 2000). Molecular and biochemical approaches have shown direct interactions between AcrA to AcrB (Zgurskaya and Nikiado 2000), AcrA to TolC (Husain *et al*., 2004; Gerken and Misra, 2004) and TolC and AcrB (Tamura *et al*., 2005; Weeks *et al*., 2010). However, direct interaction between AcrB and TolC is controversial and currently the subject of

heavy debate. In a recent study, visualization of entire tripartite complex does not support a direct interaction between TolC and AcrB; however, it is worth noting that the recombinant tripartite complex used in this study was barely functional *in vivo*, thus leaves some room as to the full validity of their microscopy data (Du *et al*., 2015).

AcrB and its Drug Binding and Translocation Pathway(s)

The trimeric AcrB protein is highly dynamic in the drug binding and translocation pathways. Each AcrB monomer assumes three distinct conformational states during the rotation-peristaltic cycle (Seeger *et al*., 2006; Murakami *et al*., 2006). Regions of the AcrB monomer in the drug binding periplasmic domain (PD) rotates through three conformational states: access (A); binding (B) and extrusion (E) (Seeger *et al*., 2006; Murakami *et al*., 2006). This rotation is triggered by the proton relay network in the transmembrane domain (TMD). As the monomers proceed through the conformational states, the substrate travels through the defined pathway within each monomer. The drug translocation pathway begins with the access monomer, which has three entrances or channels: two facing the inner membrane and inner membrane/periplasm interface and one facing solely the periplasm (Murakami *et al*., 2006; Seeger *et al*., 2006; Husain *et al*., 2011). Once the substrate has entered the access monomer, it is deposited in the proximal drug binding pocket, which is a large opening near the entrances. The second drug binding pocket, which is also known as the distal or the deep pocket, is closed in access monomer. However, it has been shown that depending on the size of a substrate, a substrate can reach the distal pocket while in the access monomer (Nakashima *et al*., 2011; Eicher *et al*., 2012). For example, low molecular weight substrates like monocyclin

can enter directly into the distal pocket (Nakashima *et al*., 2011). Large molecular weight substrate like erythromycin will first enter the proximal pocket, and then as the access monomer shifts to the binding monomer conformation, it will move to the distal pocket (Nakashima *et al*., 2011). After the binding monomer shifts to the extrusion or exit monomer, the substrate then travels through the funnel-like opening near the upper-center portion of AcrB where it exits towards TolC for expulsion out of the cell.

The AcrB drug binding and translocation pathway(s) are well-known for its promiscuity that allows for binding and efflux a broad spectrum of antibiotics and other substrates such as dyes, detergents (Nishino and Yamaguchi, 2001; Li *et al*., 2015), solvents (Tsukagoshi and Aono, 2000) bile salts, free fatty acids (Rosenberg *et al*; 2003) and metabolites (Ruiz and Levy, 2014). The mechanistic basis for promiscuity of AcrB is largely unknown since the inner anatomy and mechanisms of the drug binding and translocation are not well understood. Therefore, the endeavor to identify specific functional residues that affects the drug binding pockets and translocation of substrates is top priority. There are a number of investigations that use computational modeling and experimental approaches to unveil the properties and anatomy of the drug pockets and pathways. It is thought that promiscuity of AcrB is due to several key residues that line the drug translocation pathway and drug binding pockets. Some residues have already been identified in the drug pockets and pathways. For example, phenylalanine residues 136, 178, 610, 615, 617 and 628 were identified via modeling to form a hydrophobic cluster in between the proximal and distal pockets (Seeger *et al*., 2006). Some of these residues make direct interaction with substrates. However, one residue Phe-610 (F610) was shown not to bind substrates directly, but when substituted with alanine (F610A)

caused a drug hypersensitive phenotype thus revealing its importance in AcrB function (Bohnert *et al.,*2008). It was later shown that F610A mutation altered the binding pocket position and hindered binding monomer from transitioning to extrusion monomer (Vargiu *et al*., 2011). F617, known as the "switch loop" residue, is unique in that its orientation is coupled to the proton motive force and this determines what state the monomer is in. When the adjacent residue Gly-616 (G616) was substituted to Asn (G616N) the switch loop's flexibility was hindered thus resulting in the loss-of-conformational change from access to binding monomer (Cha *et al*., 2014). There are additional residues that are essential for AcrB activity, but are not located within the drug binding pocket. The proton relay network, which drives the conformational switch, has at least five key residues: Asp-407, Asp-407, Lsy-940, Arg-971 and Thr-987, all of which are located in the TM domain. These residues influence the drug binding/translocation pathway by supplying energy for conformational transition.

A study carried out by Soparkar *et al*. (2015) identified seven functionally significant residues/sites in the drug binding and translocation pathway of AcrB. These residues/sites are the focus of this investigation. Henceforth, the term "site(s)" refers to the position of the residue in the amino acid sequence of AcrB. As mentioned above F610 is a part of the phenylalanine cluster located within the pathway itself, but has not been shown to make direct contact with substrates (Bohnert *et al*., 2008). When substituted with alanine, F610A causes hypersensitivity to a number of substrates. Soparkar *et al*. utilized the hypersensitivity phenotype of F610A AcrB mutant to develop a positive selection strategy. By exposing AcrB F610A to selective pressures (i.e. antibiotics) they sought to isolate antibiotic resistant AcrB variants. The increase in resistance was due to

secondary mutations that suppress the hypersensitive phenotype conferred by F610A. The secondary mutations, or henceforth suppressors, identified were Tyr-49-Ser (Y49S), Val-127-Ala (V127A), Val-127-Gly (V127G), Asp-153-Glu (D153E), Gly-288-Cys (G288C), Leu-486-Trp (L486W), Phe-453-Cys (F453C). These substitutions in the presence of F610A, were able to alter the binding pocket or translocation pathway in such a way to reverse the defect caused by F610A.The mechanisms by which these substitutions overcome the defect were only minimally investigated. In this work, further research was carried out to examine the mechanisms by which suppressors function.

Rationale and Goals of this Work

The AcrB efflux pump, the primary exporter of antibiotics in *Escherichia coli*, has very broad substrate specificity. Its ability to recognize and export numerous unrelated substrates is thought to be due to highly flexible drug binding pockets and multiple drug translocation pathways. However, the complete anatomy of the drug binding pocket and translocation pathways are not fully clear. Several studies have identified AcrB residues that directly or indirectly influence the translocation pathway (Bohnert *et al*., 2008; Husain and Nikaido 2010; Koayashi *et al*., 2014; Nakashima *et al*., 2011; Eicher *et al*., 2012; Soparkar *et al*., 2015). The residues identified by Soparkar *et al*. (2015) will be further characterized in this study. The AcrB alterations examined here are: Y49S, V127G, D153E, G288C, and L486W. The first four residues/sites are located in the periplasmic domain, while the last, L486W is located in the transmembrane domain (Fig. 1).

The objective of this study is to characterize these suppressor residues in more detail to further investigate their abilities to overcome the defect caused by F610A. Three major aims were undertaken to characterize the suppressor residues. The first aim concerned the side chains specificities at a particular suppressor site. The second aim was to determine whether suppressors residues employ the same or different mechanisms to overcome the F610A defect. The third aim was to characterize the effects of efflux pump inhibitors on AcrB variants carrying suppressor alterations. Each aim is described in its corresponding chapter.

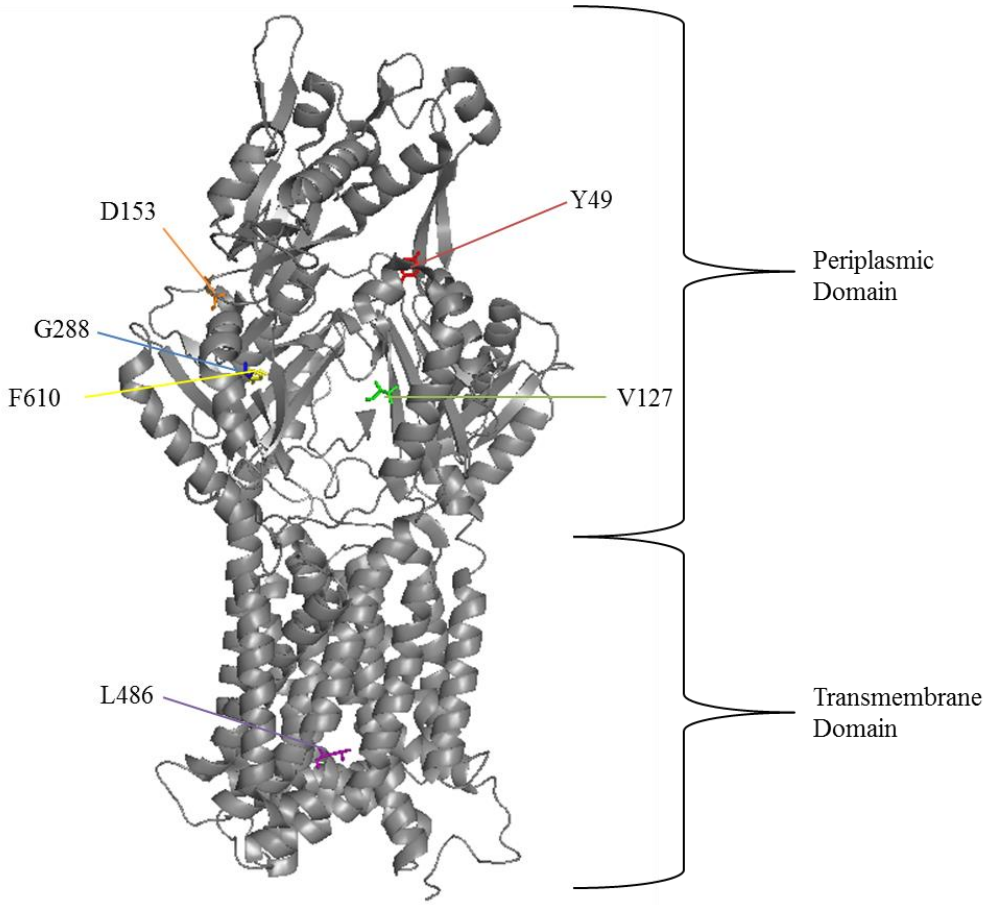

FIGURE 1: An AcrB monomer with suppressor mutations AcrB X-ray crystallography structure acquired from Protein Data Bank (2GIF). Locations of AcrB suppressors and position of F610 are depicted in color.

CHAPTER 2

AIM 1: SIDE-CHAIN SPECIFICITY OF SUPPRESSORS

Of the seven suppressors—Y49S, V127A, V127G, D153E, G288C, F453C and L486W—some had drastic changes in side chain properties, while others were very similar to the native residue. We asked whether drastic changes in the side chain properties are necessary for suppression. The two suppressors examined here were Y49S and D153E. These suppressors were chosen based on drastically differing side chain characteristics from the original residue to overcome the F610A defect.

Suppressor Y49S

Y49 is located near the exit tunnel of AcrB (Fig. 1). The native tyrosine (Y) residue has a large side chain with a benzene ring and a hydroxyl group. The suppressor substitution of serine (S) on the other hand has a small side chain with only the hydroxyl group. At this site, it was hypothesized that to overcome the F610A defect, a residue with a small side chain may be preferred so as to reduce spatial hindrance. To test this hypothesis, two variants were created via site-directed mutagenesis: Y49A and Y49F in the F610A background. The first variant contains an alanine (A) substitution and the second replaces Y with phenylalanine (F). Alanine, with only a small side chain (a methyl group) resembles serine in terms presenting low spatial hindrance, while phenylalanine with a large side chain is similar to the original tyrosine residue in terms of high spatial hindrance. If the side chain volume is the main determinant of suppression, then we predict that alanine substitution at Y49 will be able to suppressor F610A's

defect. In contrast, the phenylalanine substitution at Y49 is expected not to be able to reverse the F610A defect just as the native tyrosine residue. The real-time NPN efflux and minimum inhibitory concertation (MIC) assays were used to characterize the mutants.

The NPN efflux rates were calculated as changes in the NPN fluorescent intensity (arbitrary units) over time in seconds (Δa.u./Δs) (Fig. 2; Tables 1 and 2). The F610A+Y49A mutant had an efflux rate of -3.42±0.16 Δa.u./Δs and this rate was very similar to that of the F610A+Y49S mutant (-3.31±0.17 Δa.u./Δs). Moreover, these rates were nearly threefold better than that of the F610A mutant (-1.37±0.071 Δa.u./Δs). In contrast to Y49S, the presence of an Y49F substitution in the F610A background only modestly improved efflux rate (-2.03±0.23 Δa.u./Δs compared to -1.37±.07 of F610A). The $t_{efflux\ 50\%}$ values mirrored the efflux rates trends for the mutants (Table 1).

The MIC data in general followed the similar pattern as the NPN efflux assay. The alanine substitution at Y49A and the original suppressor Y49S both had identical MIC values for novobiocin (64 μg/mL) and erythromycin (32 μg/mL). These values are four (for novobiocin) and eight (for erythromycin) fold higher than the MIC values of the F610A mutant. It should be noted that any MIC value of two-fold or higher is considered significant. Unlike the Y49S and Y49A substitutions, the Y49F substitution only made a modest improvement in MIC values, increasing them by twofold over that displayed by the F610A mutant (Table 3).

The effects of various substitutions at site 49 of wild-type AcrB in the absence of F610A were examined to see how they influence wild-type function. As seen in Figure 2B and Table 2, the original suppressor Y49S displayed biphasic kinetics. That is, an

initial slow efflux rate in the first 25 s followed by a faster rate in the next 25 second. In spite of this, however, MIC values were similar to wild-type (Table 4). In contrast, Y49A and Y49F substitutions acted very similarly to wild-type both in NPN and MIC assays. Together, these data showed that while the natural suppressor substitution of Y49S works best in the F610A background, by itself it produces the most deleterious effect on AcrB structure/function. Moreover, the data suggested that a smaller side chain residue is preferred at site 49 for suppressing the F610A defect.

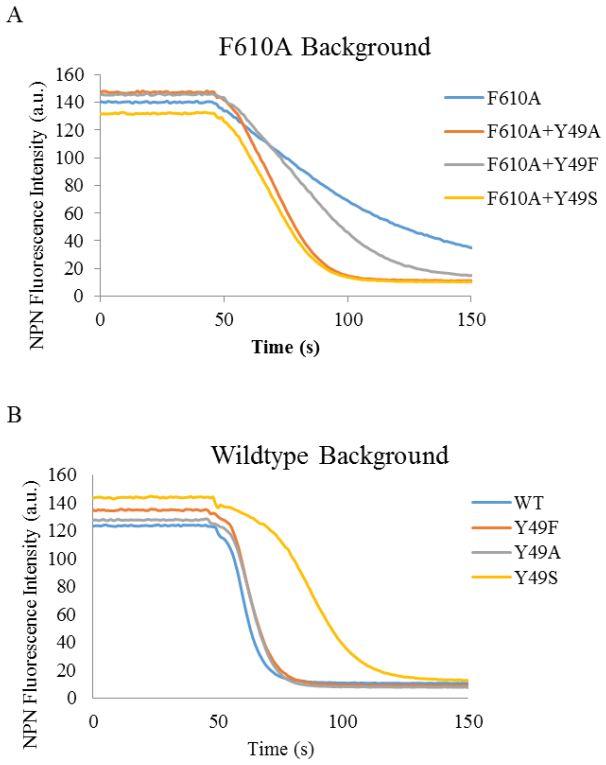

FIGURE 2: NPN efflux assays of Site 49 mutant variants. Bacterial cells were treated with CCCP to de-energize the inner membrane thus deactivating AcrB, then treated with NPN fluorescence dye. NPN dye integrate within the cellular membrane and emits with higher fluorescence intensity. After the addition of 50 mM of glucose at 100s time point, the cellular membrane is re-energized and AcrB efflux activity is restored. The negative slope reflects efflux rate of AcrB exporting NPN dye into the aqueous solution. **A.** The suppressor Y49S, which overcome the F610A drug binding defect, significantly improved NPN efflux. Two additional mutants, carrying Y49F and Y49A in the F610A background, were tested. **B.** All AcrB substitutions shown in A were also tested in wild-type AcrB background. The native suppressor Y49S displayed a biphasic efflux rate, meaning in the first 25 seconds the rate was much slower than in the next 25 seconds. These rates were significantly lower than that of wild-type or the other two variants, Y49A and Y49F. Quantitative values of efflux rate are listed in Tables 1-4.

TABLE 1 NPN Efflux rates and $t_{efflux\ 50\%}$ values for Site 49 in F610A background. Values were derived from graphs depicted in Fig 2A.

Mutants Variants	NPN Efflux	
	Efflux rate (Δa.u/Δs)	$t_{efflux\ 50\%}$ (s)
F610A	-1.37±0.071	48.30± 1.50
F610A+Y49A	-3.42±0.16	20.80±1.26
F610A+Y49F	-2.03±0.23	34.55± 2.38
F610A+Y49S	-3.31±0.17	20.05± 4.08

TABLE 2 NPN Efflux rates and $t_{efflux\ 50\%}$ values for Site 49 in wild-type background. Values were derived from graphs depicted in Fig 2B.

AcrB Mutants Variants	NPN Efflux	
	Efflux rate (Δa.u/Δs)	$t_{efflux\ 50\%}$ (s)
(AcrB-WT)	-8.41±1.52	11.17± 1.64
Y49S	-1.19±0.38; -3.42±0.14[a]	38.80± 5.91
Y49A	-7.28±1.24	25.05±0.82
Y49F	-7.77±1.14	24.80±2.06

[a] Two efflux rates represent the biphasic slope, as shown in Fig. 2B.

TABLE 3 MIC values for Site 49 in F610A background. The mutants were used to examine side chain characteristics at site 49 of AcrB-F610A background.

AcrB Mutants Variants	MIC (μg/mL)	
	Novobiocin	Erythromycin
F610A	16	4
F610A+Y49A	64	32
F610A+Y49F	32	8
F610A+Y49S	64	32

TABLE 4 MIC values for Site 49 in wild-type background. The mutants used to examine side chain characteristics at site 49 of AcrB wild-type background.

AcrB substitution (Single Mutants)	MIC (μg/mL)	
	Novobiocin	Erythromycin
(AcrB-WT)	128-256	256
Y49S	128-256	128
Y49F	128-256	256
Y49A	128-256	128-256

Suppressor D153E

Similar approaches were carried out to analyze site 153 just as described above for site 49. Here, instead of the side chain volume, the side chain charge/polarity was evaluated. The site 153 is located near the drug binding pocket (Fig. 1). The native residue is aspartic acid (D) whose side chain is negatively charged. Surprisingly, its substitution with another negatively charged residue glutamic acid (E) overcomes the F610A-conferred hypersensitivity phenotype. In other words, even though both residues are negatively charged, they yield drastically different effects on the function of the mutant AcrB protein. To analyze this site further, two additional variants were generated by SDM: D153A and D153K in F610A and wild-type backgrounds. The former has an alanine (A) substitution, thus creating a neutral and small side chain at this site. The latter mutant contains a lysine (K) residue, thus replacing the negative charge of the native residue at this site with a positive charge.

The real-time NPN efflux and MIC assays were employed to characterize these mutants. The NPN efflux assay data showed slight differences between the mutants. The original suppressor substitution of D153E and the lysine substitution at this site (D153K) had the similar efflux rates of -2.34±0.03 Δa.u./Δs and -1.97±0.26 Δa.u./Δs, respectively. The $t_{efflux\ 50\%}$ value of F610A+D153K (46.80± 3.77 s) was, however, very similar to the hypersensitive mutant F610A (48.30± 1.50 s). The alanine substitution at this site (D153A) had a lower efflux rate of -1.44±0.178 Δa.u./Δs, which was close to the value of -1.37±0.06 Δa.u./Δs displayed by the hypersensitive mutant F610A without any suppressor substitution. The $t_{efflux\ 50\%}$ value of F610A+D153A was higher than F610A mutant (Table 5).

In contrast to the data from the NPN efflux assay, the MIC data showed that both variants (D153A and D153K) in the F610A background significantly improved AcrB function. For novobiocin, both elevated MICs by twofold but for erythromycin they elevated MICs by eightfold (D153A) and fourfold (D153K) over that of the F610A mutant alone. In general, the mutant with the original suppressor substitution (D153E) performed better than the other two variants and this is consistent with the NPN efflux data. The fact that the D153A+F610A mutant did slightly better than the D153K+F610A mutant in the MIC assay in contrast to the NPN efflux assay may reflect a slightly different behavior of the two mutants against different substrates used in the two assays. In addition, the kinetic (NPN efflux) versus steady-state (MIC) measurements may reveal slightly different functional behaviors of the mutants.

The effect of various alterations at site 153 in the absence of F610A was examined to see how these changes by themselves influence wild-type AcrB function. The original suppressor alteration of D153E slightly reduced the NPN efflux rate compared to the wild-type strain (Fig. 3B and Table 6). In contrast, both D153A and D153K more drastically lowered the NPN efflux rate over the wild-type strain, indicating that they impose a substantial structural/functional perturbation on the wild-type AcrB protein compared to the natural D153E suppressor alteration. Unlike the obvious quantitative differences in NPN efflux rates displayed by the three 153 site alterations, they behaved very similarly in the MIC test, thus highlighting the significance of conducting independent tests to reveal possible functional differences caused by various alterations in AcrB.

Both sites 49 and 153 require a particular side chain property to overcome the defect caused by F610A alteration within the drug binding pocket. The data for site 149 clearly indicated a preference for small side chain for suppression. However, the preference at site 153 was not immediately obvious because both the native and suppressor side chains were negatively charged. It is possible that besides the negative charge, which does not appear to be strictly required, a slightly lager glutamate over aspartate may initiate necessary interactions required for suppression. Regardless of the exact mechanism of suppression, the data of suppressor alterations in wild-type AcrB indicate significant structural changes that are beneficial in the mutant background but detrimental in the wild-type background.

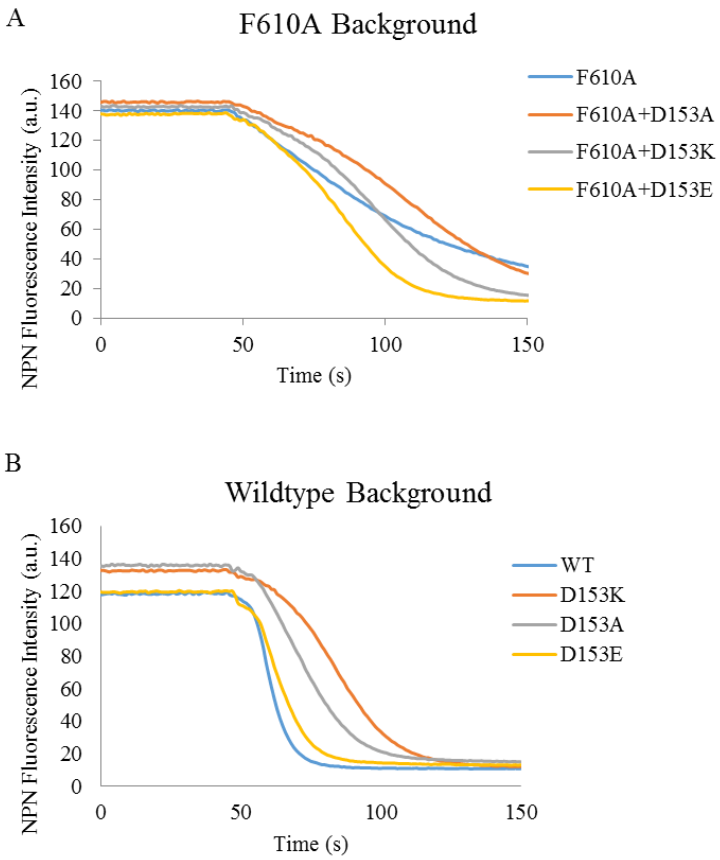

FIGURE 3: NPN efflux assays of Site 153 mutant variants. NPN efflux assays examining the polarity characteristics of site 153. The native residues of aspartic acid (D), a negatively charged residue, was substituted for another negatively charged residue glutamic acid (E). The mutant variants generated replaced D153 a positive charged residue lysine (K) and a neutral residue alanine (A). **A.** In the presence F610A, the native suppressor D153E and the mutant variant D153K had similar efflux rates; however, D153K had similar $t_{efflux50\%}$ to F610A. D153A had efflux rate similar to F610A and a greater $t_{efflux50\%}$. **B.** In the absence of F610A defect, the negatively charged residues D153 and E153 were preferred over others, with the positively charged residue was least preferred residue at this site. Quantitative values of efflux rates and $t_{efflux50\%}$ are listed in Tables 5-8.

TABLE 5 NPN Efflux rates and $t_{efflux\ 50\%}$ values for Site 153 in F610A background. Values were derived from graphs depicted in Fig 2A.

	NPN Efflux	
AcrB Variants	Efflux rate (Δa.u/Δs)	$t_{efflux\ 50\%}$ (s)
F610A	-1.37±0.07	48.30± 1.50
F610A+D153A	-1.44±0.18	61.55± 3.00
F610A+D153K	-1.97±0.26	46.80± 3.77
F610A+D153E	-2.34±0.027	34.05±1.15

TABLE 6 NPN Efflux rates and $t_{efflux\ 50\%}$ values for Site 153 in wildtype background. Values were derived from graphs depicted in Fig 2B.

	NPN Efflux	
AcrB Variants	Efflux rate (Δa.u/Δs)	$t_{efflux\ 50\%}$ (s)
AcrB-WT	-8.41±1.52	11.17± 1.64
D153A	-3.28±0.65	38.05±1.00
D153K	-2.96±0.47	45.05±0.82
D153E	-4.76±1.18	15.30±3.30

TABLE 7 MIC values for Site 153 in F610A background. The mutants used to examine side chain characteristics at site 153 of AcrB wildtype background.

	MIC (μg/mL)	
AcrB Variants	Novobiocin	Erythromycin
F610A	16	4
F610A+D153A	32	32
F610A+D153K	32	16
F610A+D153E	64	32-16

TABLE 8 MIC values for Site 153 in wildtype background. The mutants used to examine side chain characteristics at site 153 of AcrB wildtype background.

	MIC (μg/mL)	
AcrB Variants	Novobiocin	Erythromycin
(AcrB-WT)	256/128	256
D153A	256/128	128
D153K	128/64	128/64
D153E	256/128	64

CHAPTER 3

AIM 2: MECHANISM OF SUPPRESSION BY PERIPLASMIC AND TRANSMEMBRANE DOMAIN ALTERATIONS

As mentioned in above in Aim 1, the seven suppressors of the AcrB mutant (F610A) mapped in six locations throughout the AcrB protein. Five mapped within the periplasmic domain (PD) and two within the transmembrane domain (TMD). The PD suppressors were expected to arise since F610A directly affects the periplasmic drug binding pocket. The TMD suppressors were less expected because they are a long distance from the known drug binding pockets, and the main function of TMD is to energize the protein via the proton relay network. Therefore, suppressors mapping within the TMD likely overcome the PD defect through an indirect mechanism. All suppressors increased drug resistance as shown in their MIC values and NPN efflux rates (Soparkar *et al*., 2015). However, unlike the PD suppressors, the TMD suppressors were not able to improve nitrocefin efflux where substrate affinity was also measured (Soparkar *et al*., 2015). Since some suppressors were able to improve nitrocefin affinity while others could not, this indicates that at least two different mechanisms exist to overcome F610A defect. In this aim, we further characterized some of these suppressors to determine the mechanism by which they act. The following rationale was used to discern the mechanisms: if PD and TMD suppressors act through the same mechanism, their combined effects in reversing the F610A defect may not be additive. One other hand, if the two suppressors act through independent mechanism then their combined effects may

be additive. A third scenario is possible where by the two suppressors may interfere with each other's mechanism, thus produce a negative phenotype when combined.

To test these possibilities, triple mutants were generated via site-directed mutagenesis. An individual PD suppressor mutation was introduced into the F610A mutant *acrB* gene already bearing one of the TMD suppressors. The phenotypes of the triple mutants were then compared with the double mutants containing the individual suppressors in the F610A background. The PD suppressors used in this aims were V127G, D153E, G288C; while L486W was used as the TMD suppressor. A triple mutant with PD suppressor Y49S and TMD suppressor L486W could not be created despite repeated efforts.

PD Suppressor V127G and TMD Suppressor L486W

The PD suppressor alteration of V127G is located within the PN1 sub-domain of the AcrB protein. This location is not directly within the drug binding pocket (Fig. 1). The NPN assays carried out with this triple mutant showed biphasic efflux kinetics (Fig. 4; Table 9). That is, an initial slow efflux rate (-0.93±0.19 Δa.u./Δs) in the first 25 s followed by a faster rate (-2.10±0.18 Δa.u./Δs) in the next 25 second. Both rates were lower than the rates of the two double mutants, F610A+V127G (-2.72±0.34 Δa.u./Δs) and F610A+L486W (-2.97±0.18 Δa.u./Δs). Furthermore, the $t_{efflux\ 50\%}$ value was significantly higher for the triple mutant than the double mutant (Table 9). These data suggest that the PD suppressor V127G and the TMD suppressor L486W act somewhat antagonistically with respect to their abilities to overcome the NPN efflux defect conferred by F610A.

Unlike the NPN efflux assays, the MIC data were less clear with regards to establishing the antagonistic relationship between V127G and L486W (Table 10). In this assay, the MIC values of the triple mutant for both novobiocin and erythromycin improved to resemble that of the F610A+V127G mutant, showing the dominance of the V127G-mediated suppression over that mediated by L486W.

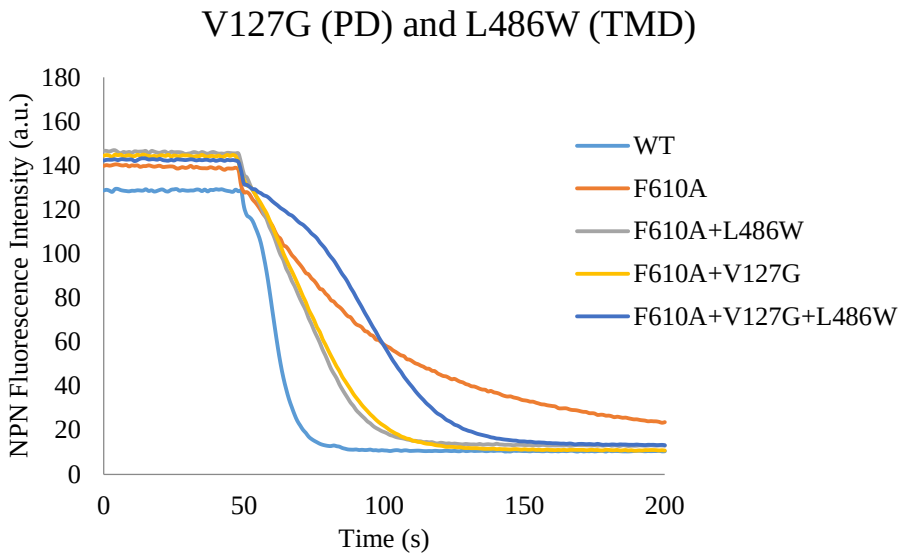

FIGURE 4: NPN efflux assays of periplasmic V127G and transmembrane L486W mutants. The triple mutant containing the periplasmic domain (PD) suppressor V127G, transmembrane domain suppressor (TMD) L486W and the hypersensitive mutant F610A showed to be more defective than the double mutants. The triple mutant also showed a biphasic slope. The first ~25s had an efflux rate nearly equal to the F610A alteration, then the following ~25s the efflux rate increased, yet still not as efficient as the double mutants. The data showed an antagonistic behavior of V127G and L486W in the F610A background. Quantitative values of efflux rates and $t_{efflux50\%}$ are listed in Table 9.

TABLE 9 Efflux rates and $t_{efflux\ 50\%}$ values of PD suppressor V127G and TMD suppressor L486W mutant variants

AcrB Variants	NPN Efflux	
	Efflux rate (Δa.u/Δs)	$t_{efflux\ 50\%}$ (s)
WT	-8.00± 0.72	11.55± 1.29
F610A	-1.20±0.12	39.55±5.07
F610A+L486W	-2.97±0.18	22.30± 2.22
F610A+V127G	-2.72±0.34	24.38± 4.08
F610A+V127G+L486W	-0.93±0.19; -2.10±0.18[a]	43.68± 4.90

[a] The two efflux rates from the biphasic slope of the triple mutant is deduced from Fig. 4.

Table 10 Minimum Inhibitory Concentration (MIC) values of periplasmic suppressor V127G and transmembrane suppressor L486W mutants

AcrB Variants	MIC (μg/mL)	
	Novobiocin	Erythromycin
WT	128	128
F610A	8	2
F610A+L486W	32	16
F610A+V127G	64	32/64
F610A+V127G+L486W	64	32/64

PD Suppressor D153E and TMD Suppressor L486W

In contrast to the V127G and L486W combination, when the PD suppressor D153E, located in the PN2 sub-domain of AcrB, was combined with the TMD suppressor L486W in the F610A background, the outcome was additive. As shown in Figure 5 and Table 11, the NPN efflux rate (-4.54±032Δa.u./Δs) of the triple mutant F610A+D153E+L486W was higher than the double mutants F610A+D153E (-2.02 ±0.52Δa.u./Δs) and F610A+L486W (-2.97±0.18 Δa.u./Δs). Consistent with the NPN data, the simultaneous presence of the two suppressor alterations in the F610A background significantly improved the MIC values of the mutant AcrB protein for both novobiocin and erythromycin (Table 12). These data suggest that the PD suppressor (D153E) and TMD suppressor (L486W) act via independent and non-interfering mechanisms to partially reverse the F610A defect.

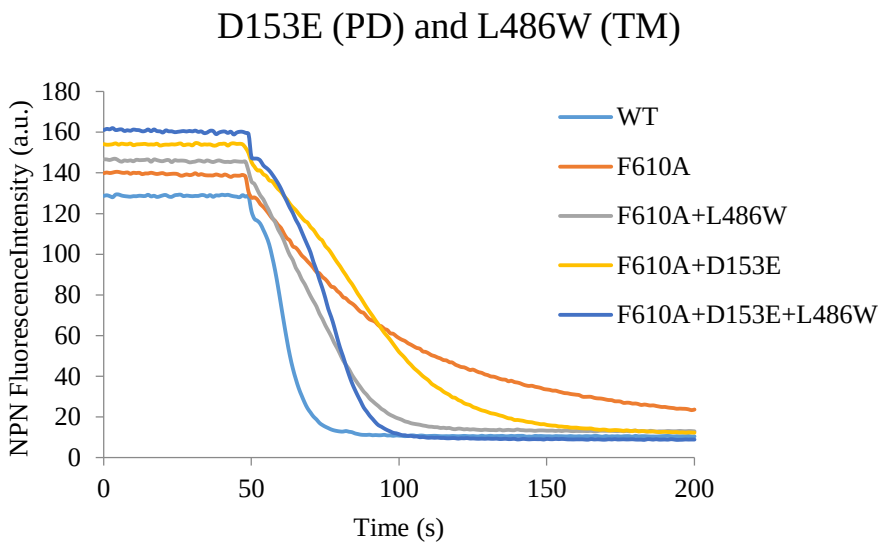

FIGURE 5 NPN Efflux assays with periplasmic D153E and transmembrane L486W mutants. The PD suppressor D153E and TMD suppressor L486W in combination with F610A demonstrated an additive effect as the rate of the triple mutant is nearly twice that of the double mutant; however, the efflux rate is not equal to wild-type, meaning there is still some defect either caused by the F610A alteration or the combined PD and TMD alterations. Quantitative values of efflux rates and $t_{efflux50\%}$ are listed in Table 11.

Table 11 NPN efflux rates and $t_{efflux\ 50\%}$ (s) of periplasmic suppressor D153E and transmembrane suppressor L486W mutant variants.

AcrB Variants	NPN Efflux	
	Efflux rate (Δa.u/Δs)	$t_{efflux\ 50\%}$ (s)
WT	-8.00 ± 0.72	11.55± 1.29
F610A	-1.20±0.12	39.55±5.07
F610A+L486W	-2.97±0.18	22.30± 2.22
F610A+D153E	-2.02± 0.52	31.38± 3.21
F610A+D153E+L486W	-4.54±0.32	24.80± 2.06

Table 12 MIC values of periplasmic suppressor D153E and transmembrane suppressor L486W.

AcrB Variants	MIC (μg/mL)	
	Novobiocin	Erythromycin
WT	128	128
F610A	8	2
F610A+L486W	32	16
F610A+D153E	32	16
F610A+D153E+L486W	64	32

PD Suppressor G288C and TMD Suppressor L486W

G288 is located directly within the distal drug binding pocket just as the F610 residue (Table 1). The triple mutant F610A+G288C+L486W had an efflux rate (-7.41±0.69 Δa.u./Δs) similar to that of wild-type (-8.00±0.72 Δa.u./Δs) and F610A+G288C (-6.42±1.07Δa.u./Δs), but significantly better than F610A+L486W (-2.97±0.18). The MIC data for erythromycin follow the similar trend as the NPN efflux data (Table 14). G288C has been shown to reverse F610A defects better than any other suppressors identified (Soparkar *et al*., 2015), suggesting that the G288C alteration creates the most preferred mechanism to overcome F610A defect. Since the F610A+G288C+L486W triple mutant displays a much better NPN efflux rate and MIC than the F610A+L486W mutant, the G288C mechanism appears to dominate over that of L486W.

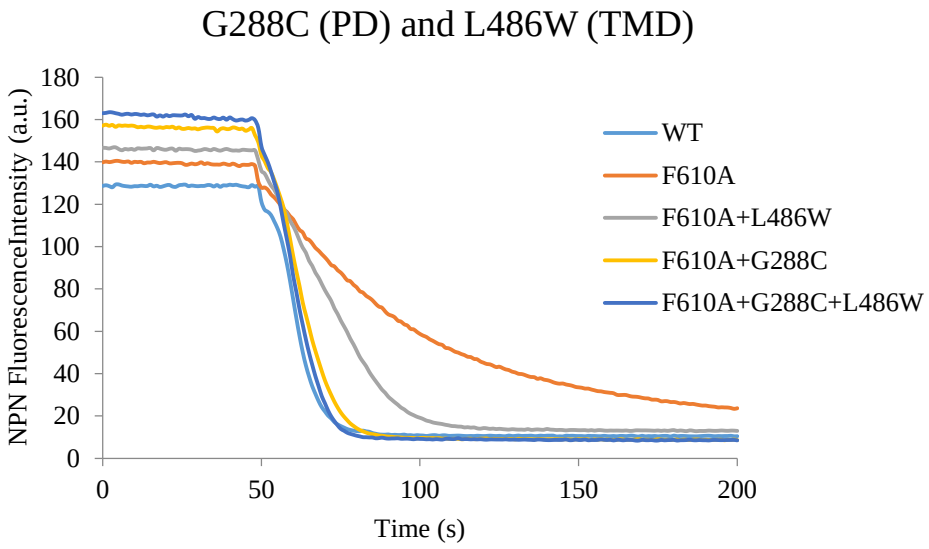

FIGURE 6 NPN Efflux assays with periplasmic G288C and transmembrane L486W mutants. The PD suppressor G288C and TMD suppressor L486W had an efflux rate and $t_{efflux\ 50\%}$ very similar to wild-type and the double mutant containing F610A and G288C alterations (Table 13). G288C suppressor has been shown previously to be the dominate suppressor out of the seven F610A suppressors (Soparkar *et al*., 2015). Its mechanism does not seem to be affected by the presence of L486W alteration. Quantitative values of efflux rates and $t_{efflux50\%}$ are listed in Table 13.

Table 13 Efflux rates of PD suppressor G288C and TMD suppressor L486W mutant variants

AcrB Variants	NPN Efflux	
	Efflux rate (Δa.u/Δs)	$t_{efflux\ 50\%}$ (s)
WT	-8.00± 0.72	11.55± 1.29
F610A	-1.20±0.12	39.55±5.07
F610A+L486W	-2.97±0.18	22.30± 2.22
F610A+G288C	-6.42±1.07	12.55± 2.08
F610A+G288C+L486W	-7.41±0.69	16.05± 3.46

Table 14 Minimum Inhibitory Concentration (MIC) values of periplasmic suppressor G288C and transmembrane suppressor L486W.

AcrB Variants	MIC (μg/mL)	
	Novobiocin	Erythromycin
WT	128	128
F610A	8	2
F610A+L486W	32	16
F610A+G288C	64	32
F610A+G288C+L486W	64	64

Effects of suppressors alterations on wild-type AcrB function

The effects of the suppressor alterations were examined in the wild-type AcrB background to see whether they influence AcrB function in the absence of F610A. To do this, the F610A alteration was converted back to wild-type F in the AcrB proteins containing either single or two suppressor alterations. The NPN efflux assays (Fig. 7A) showed V127G+L486W (-6.78 ±0.69Δa.u. /Δs) had similar rate to wild-type (-8.00 ± 0.72Δa.u./Δs). Also, the AcrB protein containing either one of the two suppressors behaved like wild-type AcrB (Fig.7A). Thus, these suppressors alterations in the wild-type background do not substantially affect AcrB function.

The presence of D153E in the wild-type AcrB protein significantly lowered NPN efflux rate, reducing it from -8.00±0.72 Δa.u./Δs for wild-type to -3.77±0.15 Δa.u./Δs with D153E (Fig. 7.B). In contrast to D153E, L486W reduced efflux rate only nominally to -6.04±0.08. When both alterations were present, the rate was similar to D153E alone (Fig 7B, Table 15). Thus, whereas both D153E and L486W produce positive effects in the F610A mutant background, their presence either alone or together is either somewhat (L486W) or significantly (D153E or D153E+L486W) deleterious in the wild-type AcrB background. The influence of D153E is dominant over the effect of L486W. Unlike the NPN efflux data, in the MIC assay, the D153E+L486W mutant behaved similarly to wild-type.

Together, it can be concluded that D153E significantly and negatively impacts wild-type AcrB function. Like D153E, the presence of G288C, one of the strongest suppressors of F610A, had a significantly negative effect on NPN efflux and this effect was dominant over that of L486W, which by itself only modestly affected efflux (Table

15; Fig. 7C). The strong negative effect is indicative of significantly structural changes within AcrB which when imposed in the F610A background have a positive effect on protein's function while enduring a negative functional effect in the wild-type AcrB background.

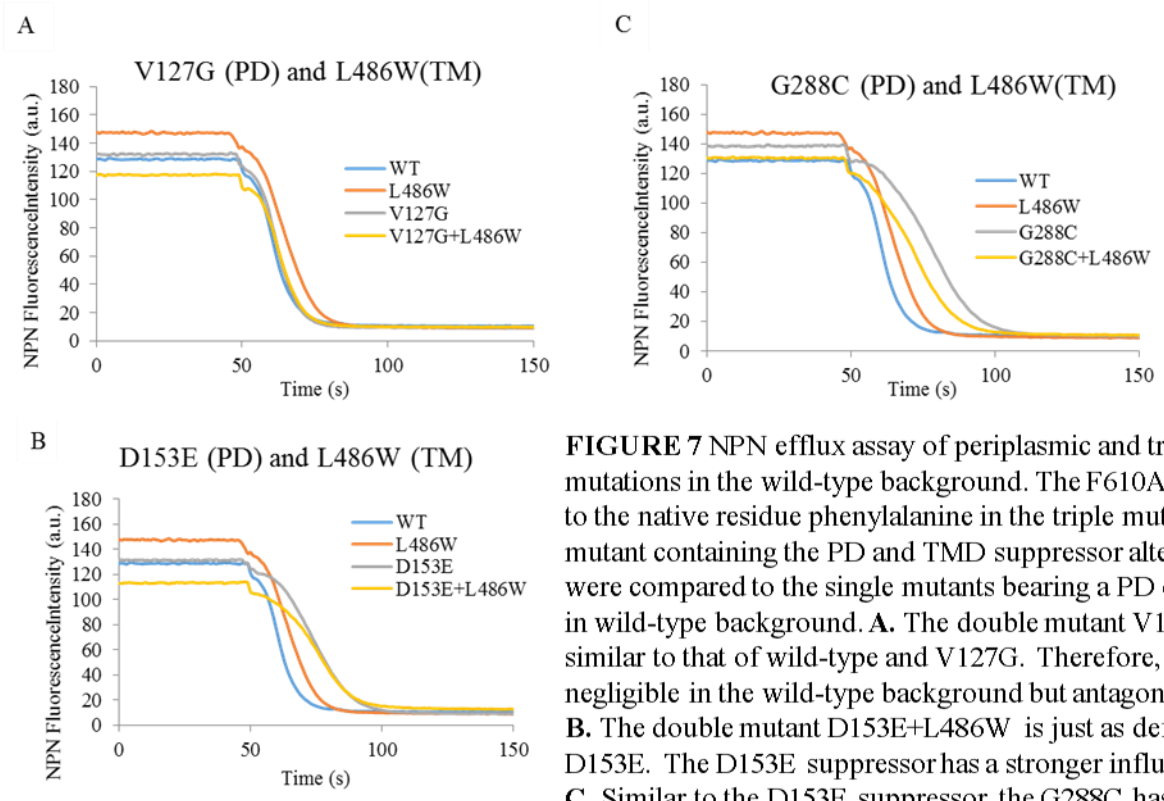

FIGURE 7 NPN efflux assay of periplasmic and transmembrane suppressor mutations in the wild-type background. The F610A alteration was changed back to the native residue phenylalanine in the triple mutant, generating a double mutant containing the PD and TMD suppressor alterations. The double mutants were compared to the single mutants bearing a PD or TMD suppressor alteration in wild-type background. **A.** The double mutant V127G+L486W had efflux rate similar to that of wild-type and V127G. Therefore, there combined effect is negligible in the wild-type background but antagonistic in the F610A background. **B.** The double mutant D153E+L486W is just as defective as the single mutant D153E. The D153E suppressor has a stronger influence on AcrB efflux activity. **C.** Similar to the D153E suppressor, the G288C has a dominant influence over the L486W suppressor on AcrB activity. Quantitative values of efflux rates and $t_{efflux50\%}$ are listed in Tables 15.

TABLE 15 Efflux rates $t_{efflux\ 50\%}$ values of PD suppressor and TMD suppressor mutant variants in wild-type background

AcrB variants	NPN Efflux	
	Efflux rate (Δa.u/Δs)	$t_{efflux\ 50\%}$ (s)
WT	-8.00± 0.72	11.55± 1.29
L486W	-6.04±0.08	14.72±1.15
V127G	-7.77±0.69	12.38±0.58
V127G+L486W	-6.78±0.69	13.05±1.83
D153E	-3.77±0.15	24.55±1.29
D153E+L486W	-3.27±0.17	26.30±1.26
G288C	-3.55±0.18	28.30±2.50
G288C+L486W	-3.98±0.39	22.80±5.50

TABLE 16 MIC values of PD suppressor and TMD suppressor mutant variants in wild-type background

AcrB variants	MIC (μg/mL)	
	Novobiocin	Erythromycin
WT	128	128
L486W	128	128
V127G	128	128
V127G+L486W	256	256
D153E	128	128/64
D153E+L486W	128	128
G288C	128	64
G288C+L486W	128	128

CHAPTER 4

AIM 3: USE OF EFFLUX PUMP INHIBITORS TO PROBE ACRB ACTIVITY

AcrB activity can be made defective by intrinsic or extrinsic means. The F610A intrinsically affects AcrB function, as determined by NPN efflux and MIC assays (see above). These defects in AcrB can be partially reversed by the intragenic suppressor alterations (Soparkar *et al*., 2015; see above). Efflux pump inhibitors (EPIs) represent extrinsic factors. EPIs, which are synthetic or natural compounds, can also decrease AcrB activities in a manner similar to the intrinsic defects, such as that caused by the F610A alteration. Both F610A and EPIs influence the same general region within the drug binding pockets of AcrB (Vargiu *et al.*, 2011; Vargiu *et al.*, 2014). The F610A alteration and EPIs, specifically phenylalanyl-arginine β-naphthylamide (PAβN) and 1-(1-naphtylmethyl)-piperazine (NMP), were shown to either block substrate binding or hinder AcrB from undergoing conformational changes necessary for drug translocation (F610A, Vargiu *et al.*, 2011; EPIs, Vargiu *et al.*, 2014).

Here, it is asked whether intragenic suppressors, which overcome the defect caused by F610A, can also overcome the defects in AcrB activity caused by PAβN and NMP. It was hypothesized that since both intrinsic and extrinsic factors negatively influence the drug binding pocket of AcrB, the intragenic AcrB suppressors may also overcome the defect caused by EPIs. On the other hand, if F610A and EPIs cause non-overlapping defects, the suppressor alterations may not reverse the defect caused by EPIs.

To test this hypothesis, NPN efflux assays were carried with AcrB variants carrying various suppressor alterations. As per protocol, glucose was added to initiate

NPN efflux. Two hundred seconds after the addition of glucose, when maximum NPN efflux was achieved, PAβN (20µg/mL) or NMP (40µg/mL) was added. The increase in NPN fluorescence intensity after the addition of EPIs reflects the efflux inhibition. If suppressor alterations prevent or reduce EPI's action on AcrB, then NPN efflux would not be as severely inhibited.

Effects of PAβN

As seen in Figure 8 and Table 17, cultures expressing wild-type AcrB displayed a modest inhibition in NPN efflux (0.490±0.108 Δa.u./Δs). Surprisingly, in cultures expressing suppressor-containing AcrB variants, NPN efflux was more severely inhibited than in wild-type AcrB cultures. These data revealed that not only the suppressor alterations were unable to overcome the PAβN-mediated inhibition, their presence made the variant AcrB proteins more sensitive to this inhibitor than the wild-type AcrB protein. Overall, the F610A suppressor mutations were unable to overcome the inhibitory effect of PAβN.

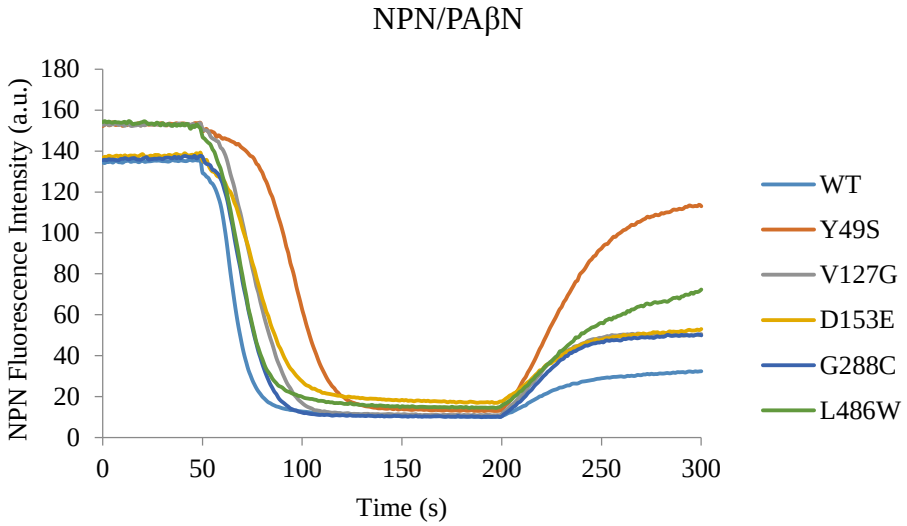

FIGURE 8: Modified NPN efflux assays with the efflux pump inhibitor (EPI) PAβN. PAβN was added after maximum efflux was reached at 200s. The graph shows that none of the F610A suppressor was able to overcome the inhibitory effects of PAβN. The rates of inhibition, i.e. the extent of positive slope, are listed in Table 17.

Table 17 Rate of inhibition via efflux pump inhibitor PAβN.

	NPN Efflux
AcrB Varaints	Rate of PAβN inhibition (Δa.u./Δs)
WT	0.490±0.108
Y49S	1.805±0.167
V127G	1.066±0.264
D153E	0.753±0.245
G288C	0.978±0.163
L486W	0.936±0.383

Of the five suppressors tested, Y49S conferred most susceptibility to PAβN, with the rate of inhibition of 1.805±0.167 Δa.u./Δs that was almost fourfold higher than that of wild-type AcrB. In first aim of this study, three Y49 mutant variants were generated to examine the effect of side chain on F610A suppression. Those results revealed that a smaller side chain at site 49 is preferred for suppression. With these results in mind, it was asked as to how various side chains at site 49 affect PAβN susceptibility. To test this, the NPN/PAβN efflux assay was performed with cultures expressing either wild-type AcrB and the Y49A, Y49F or Y49S variant. Y49A and Y49S variants behaved similarly and were more susceptible to PAβN inhibition than the Y49F variant, which behave similar to wild-type. The data revealed that the presence of large side chains (Y or F) confers greater resistance to PAβN than those with smaller side chains (S or A). These data inversely correlate with the suppression data in that small side chains are preferred for F610A suppression, but larger side chains are preferred for resistance against PAβN.

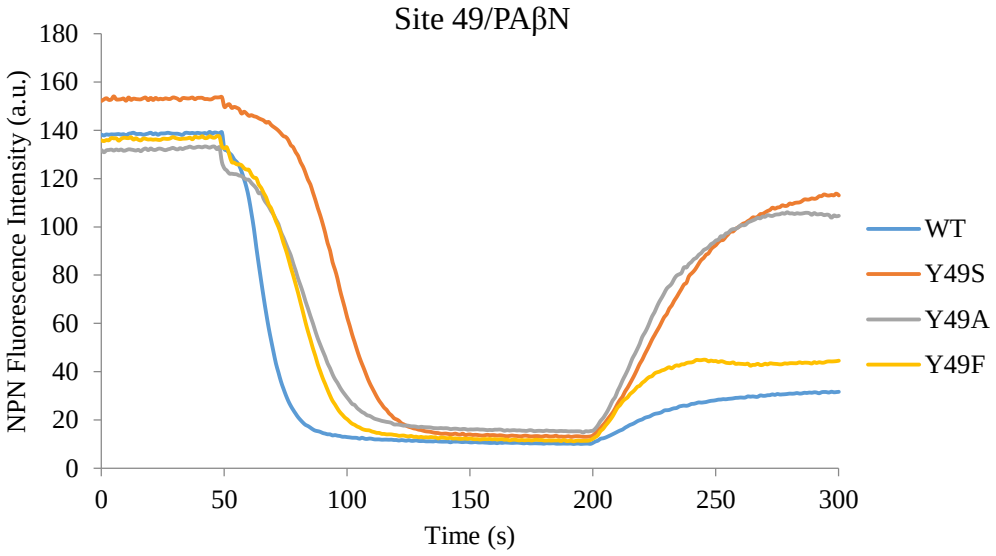

FIGURE 9: Modified NPN efflux assays with site 49 AcrB mutant variants. Y49S and Y49A mutants were strongly inhibited by the efflux pump inhibitor PAβN. The Y49F mutant was less susceptible than Y49S and Y49A, but slightly more susceptible than wild-type. Quantitative values of rates of inhibition are shown in Table 18.

TABLE 18 Rates of Inhibition for Site 49 mutant variants

	NPN Efflux
AcrB Variants	Rate of PAβN inhibition (Δa.u./Δs)
WT	0.490±0.108
Y49S	1.805±0.167
Y49A	2.12±0.29
Y49F	1.30±0.16

Effect of NMP

NMP inhibitor of AcrB protein was also used to ask if intragenic AcrB suppressors can overcome the effect of extrinsically added inhibitors. NMP (40 μg/mL) was added after the strains reached maximum NPN efflux. The NMP was found to be less effective in inhibiting AcrB than PAβN; nevertheless, a difference between wild-type and AcrB variants with suppressor alterations were noticeable (Fig. 10 and Table 19). The rate of inhibition for wild-type was 0.082±0.036 Δa.u./Δs. The suppressor mutants had inhibition rates twofold to threefold higher than wild-type. Just as the case with PAβN, the suppressor alterations were unable to overcome the inhibitory effects NMP and in fact conferred greater sensitivity than the wild-type AcrB protein.

These data indicated that the defect caused by F610A on AcrB function is not similar to that caused by EPIs. This was somewhat surprising since both F610A and EPIs used here, PAβN and NMP, are thought to affect the drug binding pocket. A closer examination of the exact binding sites of PAβN and NMP and the structural alterations caused by F610A may provide better understanding of their effects on AcrB.

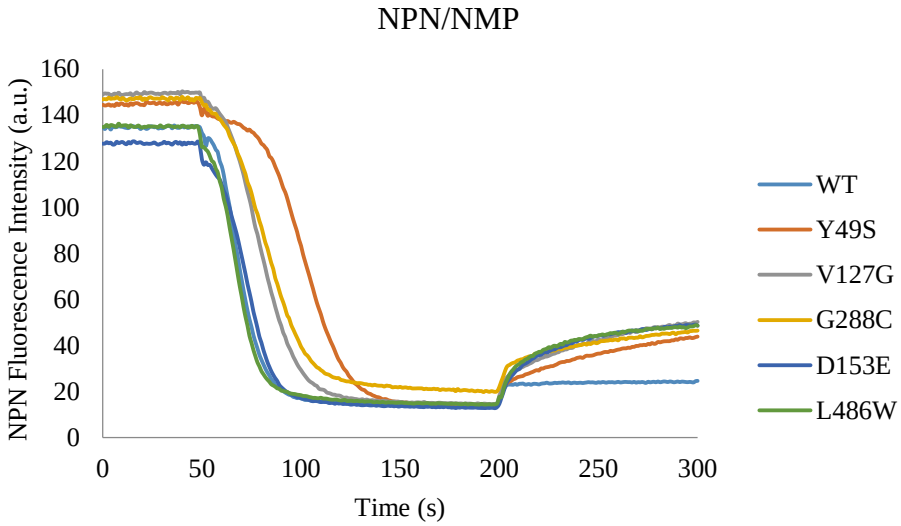

FIGURE 10: Effects of NMP-mediated inhibition of NPN efflux. Though the rates of inhibition are not as drastic as seen with PAβN (Fig 8) the conclusions are the same. The suppressor alterations were unable to over the inhibitory effects of NMP. Rates of inhibition are shown in Table 19.

Table 19 Rate of inhibition via efflux pump inhibitor NMP

	NPN Efflux
AcrB Variants	Rate of PAβN inhibition (Δa.u./Δs)
WT	0.082±0.036
Y49S	0.275±0.038
V127G	0.320±0.077
D153E	0.34±0.026
G288C	0.245±0.058
L486W	0.31±0.013

CHAPTER 5

DISCUSSION

The aim of this work was to investigate the mechanisms employed by the intragenic suppressor mutations that overcome the AcrB drug binding pocket defect caused by the F610A alteration. This alteration was shown via computational modeling to alter the dimensions of the drug binding pocket (Vargiu *et al*., 2011). Moreover, functional assays showed that the F610A alteration severely reduced the affinity of AcrB to nitrocefin; while all PD suppressors, but not TMD suppressors, reversed this defect (Soparkar *et al*., 2015). The three main aims were (1) determine side chain specificity of suppressor residues, (2) determine whether PD and TMD suppressors employ same or distinct mechanisms to over the F610A defect and (3) probe the effect of efflux pump inhibitors on mutant and wild-type AcrB proteins.

Side Chain Specificity

In this work side chain specificities of sites Y49 and D153 were characterized. (Specificity of site S288 were previously characterized in our lab by Soparkar *et al*., 2015). To test the effect of side chain volume, two AcrB variants were created bearing Y49A and Y49F alterations in the wild-type or F610A background. The NPN efflux and MIC data showed that smaller side chains of A49 and S49 are preferred over that of bulky side chains of Y49 and F49 for suppression of the F610A-mediated defect. The bulkier side chain of Y and F may be less preferred because they may cause spatial hindrances with surrounding residues to restrict drug flow. This effect is more

pronounced in the F610A background where a partial collapse in the drug binding pocket may require conformational accommodation near or at the exit channel for the resumption of drug flow. Using the measurement tool of the Pymol software program, a close interaction, via hydrogen bond, between with Y49 in the binding monomer and R239 in the extrusion monomer can be predicted in the wild-type background (Fig. 11). This interaction is not possible in the any other monomers. When Y49 is changed to serine, as in the suppressor mutant, the interaction between S49 and R239 becomes highly unlikely due to long distance between the hydrogen bonding atoms of the two residues (Fig. 11). It is possible that the lack of this molecular interaction between the binding and extrusion AcrB monomers suppresses the F610A defect. In future, this possibility can be tested by making alterations at R239. Unlike Y49, the side chain of F49 cannot engage with R239 through hydrogen bonding. Yet the two residues behave similarly in all tests performed in this work. Therefore, a bulky side chain at position 49 may also be involved in tight packing near the exit channel. This packing is disrupted when substituted with small residues S or A, which are beneficial in the F610A background (causing suppression) but somewhat deleterious in the wild-type background by affecting local folding or packing.

Unlike the Y49S substitution, D153E does not dramatically alter the side chain property at this site, yet E153 suppresses F610A defect whereas D153 does not. Glutamic acid does have a small size difference from aspartic acid because of an additional carbon in the side chain, however the two residues share the same negative charge. The site 153 is located near the drug binding pocket, but is not within the drug binding pocket. To investigate the effect of charge and volume at site 153 on F610A suppression, two

additional AcrB variants were generated bearing a D153K or D153A substitution. In contrast to D153E, the two mutant variants only slightly reversed the F610A defect as assessed by NPN efflux assays. The presence of the positively charged residue lysine at position 153 (D153K) was better at repairing the F610A defect than the neutral and small side chain (D153A). These findings indicated (1) longer polar side chains (E153 or K153) are preferred over smaller polar (D153) or apolar (A153) side chains for suppressing the F610A defect, and (2) negatively charged side chain of E153 is preferred over positively charged side chain of K153. It is currently not known why substituting D153 with a somewhat longer negative side chain of E153 is beneficial in the F610A background. The presence of any three substitutions (D153E, D153K or D153A) conferred somewhat negative effect on wild-type AcrB activity as assessed by NPN efflux assays. This indicated that conformational changes that are beneficial in the mutant AcrB background are somewhat detrimental in the wild-type AcrB backbone.

Future experiments can be designed to further examine the side chain volume and charge at site 153. To examine the effect of volume at this site, two mutants containing asparagine-153 (N153) and glutamine-153 (Q153) could be generated. The former resembles the wild-type residue aspartic acid and the latter resembles the suppressor glutamic acid. If volume is of importance to overcoming the F610A alteration, then Q153 mutant should suppress just as E153, while N153, like D153, should not. However, if charge is a necessary at this site, then neither Q153 nor N153 would overcome F610A defect.

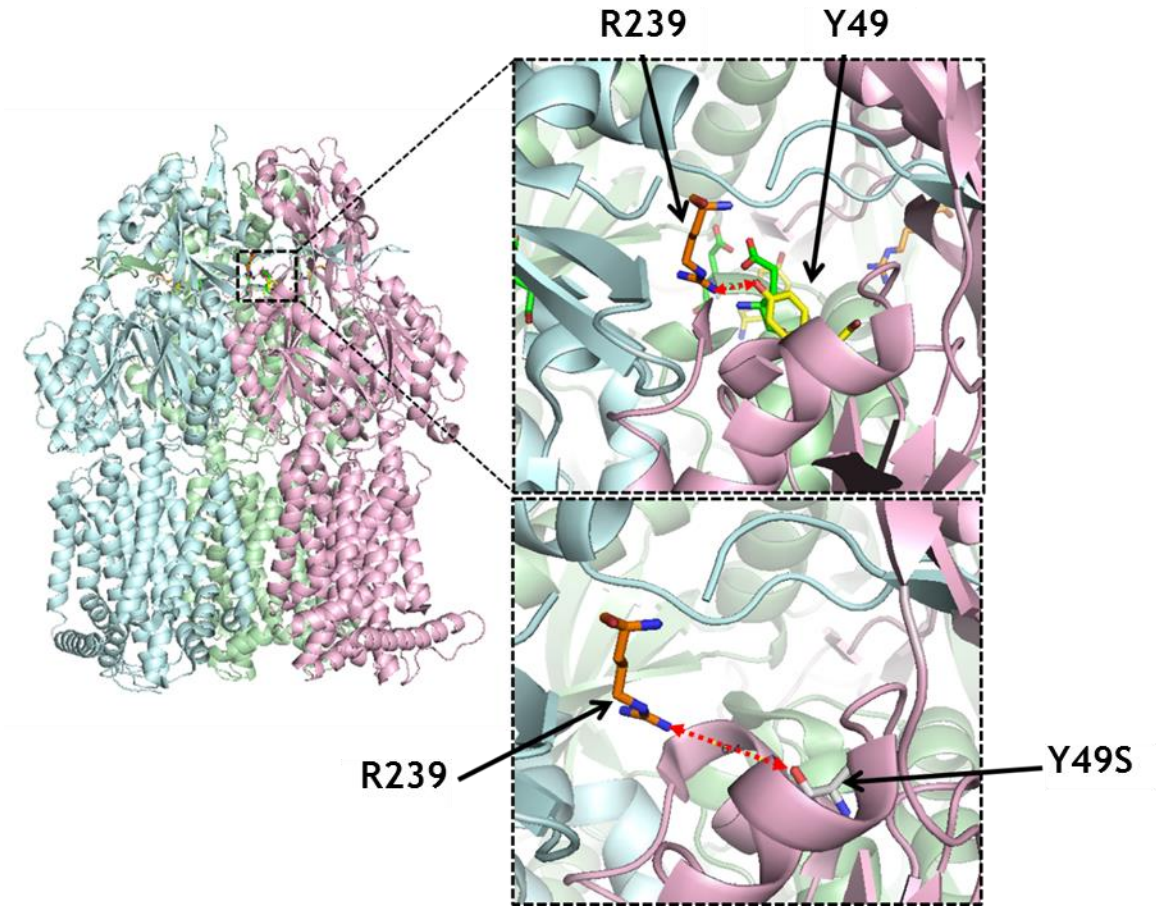

FIGURE 11 Molecular image of AcrB sites using Pymol program. A) Depict a possible interaction between the native tyrosine-49 (Y49) and arginine-239 (R239). The approximate distance of 2.7Å between the oxygen of tyrosine and a nitrogen of arginine is optimum for hydrogen bond formation. B) The site 49 was computationally mutagenized using the feature of Pymol to serine (Y49S). The distance between the oxygen of serine and a nitrogen of arginine is approximately 6.4Å, which is too far for hydrogen bond.

Suppressor Mechanisms by Periplasmic and Transmembrane Domain Alterations

Taken as a whole, the periplasmic domain (PD) suppressors—V127G, D153E and G288C—all behaved somewhat differently than the transmembrane domain (TMD) suppressor L486W in responding to the F610A defect. The PD suppressor V127G displayed an antagonistic relationship with L486W, indicating that they interfered with each other's mechanism of suppression. The L486W alteration may indirectly influence the PD and this effect is somehow negated in the presence of the PD alteration V127G. In contrast, the D153E-mediated suppression mechanism showed a positive relationship with that of the L486W alteration. This indicated that the two alterations acted independently and in a non-interfering manner to overcome the F610A defect. Finally, the G288C-mediated suppression mechanism was dominant over that of the L486W alteration, indicating that they likely acted in the same pathway.

As stated earlier, the PD binds and translocate drugs upon receiving conformation changes from the TMD which is involved in proton translocation. The F610A alteration is located in the drug binding pocket of PD. The L486W substitution likely directly influences the TMD, with or without affecting proton translocation, to then indirectly influence the PD to partly overcome the F610A defect. In contrast to L486W, the PD substitutions D153E and G288C likely directly influence the drug binding pocket to partly alleviate the F610A defect. Their mechanism of suppression is compatible with that of L486W. The V127G substitution of the PD is not in the vicinity but away from the drug binding pocket. How changes at V127 overcome the F610A defect is not known but its mechanism of suppression is not compatible that of the L486W substitution.

Effect of Efflux Pump Inhibitors on AcrB Variants Bearing Suppressor Alterations

EPIs PAβN and NMP were shown to bind to the hydrophobic trap of the drug binding pocket via computational modeling (Vargiu *et al*., 2014). These interactions are thought to induce a physical distortion that hinders substrates from binding to the drug binding pockets (Vargiu *et al*., 2014). F610A is also thought to distort the drug binding pocket (Vargiu *et al*., 2011). The mechanism of distortion caused by the intrinsic F610A substitution and extrinsic factors like EPIs may or may not be similar. In this work it was hypothesized that if EPIs distort AcrB binding pocket in a manner similar to F610A, then suppressors alterations isolated against F610A may also overcome the inhibitory effect of EPIs in a wild-type AcrB background. This hypothesis was however not supported by the data presented in this study, as none of the suppressor alterations were able to overcome the efflux defect caused two different EPIs, PAβN and NMP. In fact, the suppressor alterations made the otherwise wild-type AcrB protein more susceptible to the effects of inhibitors. This would suggest that the drug binding pocket distortion caused by F610A is not similar to the distortion caused by EPIs PAβN and NMP. Although the results of this aim did not support the hypothesis stated in this work, it does however support the conclusions made in Vargiu *et al*. (2014) pertaining to the effect of some inhibitors and the F610A substitution. Their study characterized, via computational modeling, a novel synthetic inhibitor MBX2319. This inhibitor was compared with the inhibitors D13-9001, PAβN and NMP, as well as the F610A alteration. It was concluded that inhibitors MBX2319, D13-9001 and the F610A alteration similarly influence to the hydrophobic pocket that may hinder conformational change of AcrB. In future work, the two inhibitors

MBX2319 and D13-9001 could be used to ask if the suppressors repair the effects caused these inhibitors since their mechanism of damage seems to be similar.

Conclusion

In conclusion, attempts were made in this study to gain deeper insights into the mechanism of suppression. It was discovered that specific side chain properties (e.g. size and charge) within AcrB are important for the suppression of F610A defect. Suppressor residue side chains may either produce or disrupt specific interactions with neighboring residues to allow for necessary conformational accommodation and restoration of function. The multiplicity of the suppressor mechanisms was revealed by combining PD and TMD suppressors. In some instances, the TMD and PD suppressors acted synergistically (e.g. L486W and D153), while in others they acted antagonistically (e.g. L486W and D153). This showed that despite being located in the same domain, the PD suppressors acted by somewhat different mechanisms to overcome the drug pocket binding defect. The work underscored the structural flexibility of the AcrB protein to compensate for drug binding pocket defects and further reflected the well-known promiscuity of the protein. It was also determined that the inhibitory mechanism of F610A does not overlap with the inhibitory mechanism of some efflux pump inhibitors, namely PAβN and NMP. However, other inhibitors may provide different results.

This research highlights the importance of combining genetic approaches with biochemical and structural approaches to better understand the major drug efflux mechanism. Deeper understanding of drug efflux mechanisms will aid future drug developments and novel therapeutics. For example, the investigation of the mechanism of

efflux inhibitors will possibly give rise to the development of adjuvant therapies (Nikaido and Pages, 2012; Blair *et al*, 2015; Dantzig *et al*, 2003). These therapies use EPIs in tandem with lower dosage of antibiotics to increase potency of antibiotics. Further work will be necessary for deeper knowledge of the suppressor mechanisms of AcrB residues and their implications in overcoming the effects of EPIs.

CHAPTER 6

MATERIALS AND METHODS

Bacterial Strains, Culture Conditions and Media

All strains were derived from MC4100 Δ*ara* Δ*acrAB*::scar strain and are listed in Table 20. JM109 strain was used for creation of mutants using site-directed mutagenesis. Both MC4100 Δ*ara* Δ*acrAB*::scar and JM109 were made competent via Mn^{2+}/Ca^{2+} (CCBM80) treatment as described by Hanahan *et al*. (1991). Competent cells were also stored at -80ºC until used for heat-shock transformation. Luria broth (LB) was prepared from Difco™ LB broth Lennox and purchased from Becton Dickenson. Luria broth agar (LBA) contained LB and 1.5% agar. Both LB and LBA contained 12.5ug/mL chloramphenicol (CM) to maintain plasmid. Stains were incubated at 37ºC for 16-18hrs.

Chemicals

Chloramphenicol, novobiocin and erythromycin were purchased from Sigma Aldrich. Stock concentrations were 25 mg/mL for chloramphenicol and 56.76 mg/mL for novobiocin and erythromycin. N-phenyl-1-naphthylamine (NPN), carbonyl cyanide 3-chlorophenylhydrazone (CCCP), 1-(1-napthylmethyl) piperazine (NMP), and phenylalanylarginine β-nahthylamide hydrochloride (PAβN) were also purchased from Sigma Aldrich. They were dissolved in 95% ethanol (NPN), DMSO (CCCP), HCl solution (98% of 0.1N HCl + 2% of 6N HCl) (NMP), and sterilized water (PAβN). All antibiotics and chemicals were stored at -20ºC.

Construction of Strains

Mutations were introduced in the *acrB* gene that resides in the pACYC184 plasmid alongside wild-type *acrA* gene (pACYC184 is a low-copy-number plasmid). Mutations were introduced using the Quikchange Lightening site-directed mutagenesis (SDM) kit from Agilent Technologies. Plasmid concentration for SDM was 5 ng/µL. Primers concentration were 25 ng/µL. Primers for SDM are listed in Table 21. SDM reactions were carried out using a Eppendorf Mastercycler gradient machine. The cycling parameters are indicated in Table 22. After SDM reactions, the products were transformed into competent JM109 cells. Single transformant colonies were purified on LBA+CM plates. 5mL cell cultures (in LB+CM) from these colonies were used to extract and purify plasmid using the Qiagen Spin Miniprep Kit. *acrB* from purified plasmids were then sequenced at the Arizona State University DNA lab. Sequencing primers are listed in Table 23. DNA sequences were analyzed using DNAMAN Version 3.0 from Lynnon BioSoft.

Minimum Inhibitory Concentration

MICs were carried out as described in Soparkar *et al*. (2015). Novobiocin and Erythromycin were used to determine bacterial susceptibility. MICs were performed in 96-well plates using a 2-fold dilution method. Wells were filled with LB+CM and then supplemented with the required antibiotic solution previously diluted in LB+CM. Overnight grown bacterial cultures were diluted 1:1000 (~10^6 cells/ml). Twenty uL of diluted culture was added to each well, thus making the volume of cells plus antibiotic medium to be 200µL per well. Plates were rocked gently in 37ºC incubator for 18 hours.

After incubation, optical densities at 600 nm (OD_{600}) of cultures were measured using VeraMax ELISA microplate reader from Molecular Devices. OD_{600} readings >0.1 were considered inhibitory for bacterial cells, while <0.1 were considered viable/live bacterial cells.

NPN Efflux Assay

The NPN efflux assays were carried out as described by Misra *et al*. (2015). Bacterial cells were cultured overnight for 17-18 hours, then pelleted at 3000 rpm for 10 minutes. Pellets were washed twice with phosphate buffer (20 mM potassium phosphate at pH 7.0 + 1mM magnesium chloride). Resuspended cells were then diluted 1:5 into phosphate buffer, i.e. 1 mL of bacterial culture to 4 mL of phosphate buffer. 4 mL of diluted cultures were transferred into a 15 mL-conical tube. The cells were treated for 15 minutes with 10 mM CCCP for a final concentration of 100 µM. Cells were washed twice with 4 mL of phosphate buffer each time. Cells were then treated for 15 minutes with 1 mM NPN for a final concentration of 10 µM. Then they were transferred into fluorescence cuvette and placed in Cary Eclipse Fluorescence Spectrophotometer. Setting were as follows: excitation wavelength (410 nm) emissions wavelength (340 nm) slit width (5 mm). The device plotted the intensity (a.u.) of NPN in real-time. After 100s or 50s 100 µL of 20% glucose was added. When required, inhibitors PAβN or NMP were added 200s after the addition of glucose. 40 uL of PAβN added for final concentration of 20 µg/ml and 80 uL of NMP was added for final concentration of 40 µg/mL. Fluorescence intensity was recoded for an additional 100s.

TABLE 20 Bacteria cell strains

Strain	Characteristics	Plasmids	Reference or Source
JM109	*end*A1, *rec*A1, *gyr*A96, *thi*, *hsd*R17 (rk–, mk+), *rel*A1, *sup*E44, Δ(*lac-pro*AB), [F´ *tra*D36, *pro*AB, *laq*IqZΔM15]	None	
MC4100	F- *araD139*Δ*(argF-lac)U139rpsL150 relAl flbB5301 ptsF25 deoC1 thi-l rbsR*	None	
	MC4100 Δ*ara* Δ*acrAB* scar	None	
Null	MC4100 Δ*ara* Δ*acrAB* scar	pACYC184	Soparkar *et al*., 2015
Wildtype	MC4100 Δ*ara* Δ*acrAB* scar	pACYC184 AcrAB	Soparkar *et al*., 2015
B87-018	MC4100 Δ*ara* Δ*acrAB* scar	pACYC184 ($AcrA_{WT}$ $AcrB_{F610A}$)	Soparkar *et al*., 2015
B87-022	MC4100 Δ*ara* Δ*acrAB* scar	pACYC184 ($AcrA_{WT}$ $AcrB_{Y49F}$)	This study
B87-023	MC4100 Δ*ara* Δ*acrAB* scar	pACYC184 ($AcrA_{WT}$ $AcrB_{Y49A}$)	This study
B87-024	MC4100 Δ*ara* Δ*acrAB* scar	pACYC184 ($AcrA_{WT}$ $AcrB_{D153K}$)	This study
B87-025	MC4100 Δ*ara* Δ*acrAB* scar	pACYC184 ($AcrA_{WT}$ $AcrB_{D153A}$)	This study
B87-027	MC4100 Δ*ara* Δ*acrAB* scar	pACYC184 ($AcrA_{WT}$ $AcrB_{F610A+Y49F}$)	This study
B87-028	MC4100 Δ*ara* Δ*acrAB* scar	pACYC184 ($AcrA_{WT}$ $AcrB_{F610A+Y49A}$)	This study
B87-029	MC4100 Δ*ara* Δ*acrAB* scar	pACYC184 ($AcrA_{WT}$ $AcrB_{F610A+D153K}$)	This study
B87-030	MC4100 Δ*ara* Δ*acrAB* scar	pACYC184 ($AcrA_{WT}$ $AcrB_{F610A+D153A}$)	This study
B87-032 and B87-050	MC4100 Δ*ara* Δ*acrAB* scar	pACYC184 ($AcrA_{WT}$ $AcrB_{F610A+Y49S}$)	Soparkar *et al*., 2015
B87-033	MC4100 Δ*ara* Δ*acrAB* scar	pACYC184 ($AcrA_{WT}$ $AcrB_{F610A+D153E}$)	Soparkar *et al*., 2015
B87-034 and B87-067	MC4100 Δ*ara* Δ*acrAB* scar	pACYC184 ($AcrA_{WT}$ $AcrB_{D153E}$)	This study
B87-035 and B87-68	MC4100 Δ*ara* Δ*acrAB* scar	pACYC184 ($AcrA_{WT}$ $AcrB_{G288C}$)	Soparkar *et al*., 2015
B87-036 and B87-065	MC4100 Δ*ara* Δ*acrAB* scar	pACYC184 ($AcrA_{WT}$ $AcrB_{Y49S}$)	This study
B87-037 and B87-066	MC4100 Δ*ara* Δ*acrAB* scar	pACYC184 ($AcrA_{WT}$ $AcrB_{V127G}$)	This study
B87-039	MC4100 Δ*ara* Δ*acrAB* scar	pACYC184 ($AcrA_{WT}$ $AcrB_{L486W}$)	Soparkar *et al*., 2015
B87-052	MC4100 Δ*ara* Δ*acrAB* scar	pACYC184 ($AcrA_{WT}$ $AcrB_{F610A+G288C}$)	Soparkar *et al*., 2015
B87-049	MC4100 Δ*ara* Δ*acrAB* scar	pACYC184 ($AcrA_{WT}$ $AcrB_{F610A+L486W}$)	Soparkar *et al*., 2015
B87-056	MC4100 Δ*ara* Δ*acrAB* scar	pACYC184 ($AcrA_{WT}$ $AcrB_{F610A+V127G+L486W}$)	This study
B87-053	MC4100 Δ*ara* Δ*acrAB* scar	pACYC184 ($AcrA_{WT}$ $AcrB_{F610A+D153E+L486W}$)	This study
B87-047	MC4100 Δ*ara* Δ*acrAB* scar	pACYC184 ($AcrA_{WT}$ $AcrB_{F610A+G288C+L486W}$)	This study
B87-062	MC4100 Δ*ara* Δ*acrAB* scar	pACYC184 ($AcrA_{WT}$ $AcrB_{G288C+L486W}$)	This study
B87-064	MC4100 Δ*ara* Δ*acrAB* scar	pACYC184 ($AcrA_{WT}$ $AcrB_{V127G+L486W}$)	This study
B87-065	MC4100 Δ*ara* Δ*acrAB* scar	pACYC184 ($AcrA_{WT}$ $AcrB_{D153E+L486W}$)	This study

TABLE 21 Site-directed Mutagenesis primers

Primer Name	Gene	Sequence (Forward primers)
Y49A	*acrB*	5'-CGATCTCC*GCg*TCC***gcC***CCCGGCGCTGATGCG-3'
Y49F	*acrB*	5'-CGATCTCC*GCg*TCC***TtC***CCCGGCGCTGATGCG-3'
D153A	*acrB*	5'-GCACCATGACGC*AaG*AG***Gcg***ATCTCCGACTACGTGG-3'
D153K	*acrB*	5'-GGCACCATGACGC*AaG*AG***aAa***ATCTCCGACTACGTGGCG-3'
L486W	*acrB*	5' CGGTACTGGTGGCG***TgG***ATCCTGACT*CCt*GCTCTTTGTGCC-3'
A610F	*acrB*	5'-CGTTGAGTCGGTGTTCG***CgG***TTAACGGCTTCGGC-3'

Note: Bolded underline nucleotides are the mutated residue while the non-bolded underline nucleotides are silent mutations made to maintain annealing temperatures and/or GC contents.

TABLE 22 Site-Directed Mutagenesis cycling parameters

(18 cycles)	Temperature (ºC)	Time (minutes:seconds)
1	95	2:00
2	95	:20
3	60	:10
4	68	4:30

TABLE 23 Sequencing primers

Primer name	Gene	Sequence
AcrB-F1 (sites 49, 127, 153)	*acrB*	5'-CCATTATCATCATGTTGGCAGG -3'
AcrB-F3 (site 288)	*acrB*	5'- TCGAAGATTGAGCTGGGTGG -3'
AcrB-F4 (site 486)	*acrB*	5'- CCATCGGCCTGTTGGTGG -3'
AcrB-F5 (site 610)	*acrB*	5'- GCACCACTACACCGACAGC -3'

REFERENCES

Aarestrup, F. M., A. M. Seyfarth, H. D. Emborg, K. Pedersen, R. S. Hendriksen, and F. Bager. 2001. Effect of abolishment of the use of antimicrobial agents for growth promotion on occurrence of antimicrobial resistance in fecal enterococci from food animals in Denmark. Antimicrob. Agents Chemother. 45:2054-2059

Abraham, E. P., and E. Chain. 1940. An enzyme from bacteria able to destroy penicillin. Nature. 146:837.

Alanis, A. J. 2005. Resistance to antibiotics: are we in the post-antibiotic era? Arch. Med. Res. 36:697-705.

Aminov, R. I. 2010. A brief history of the antibiotic era: lessons learned and challenges for the future. Frontiers in Microbiology. 1:134.

Blair, J. M., H. E. Smith, V. Ricci, A. J. Lawler, L. J. Thompson, and L. J. Piddock. 2015. Expression of homologous RND efflux pump genes is dependent upon AcrB expression: implications for efflux and virulence inhibitor design. J. Antimicrob. Chemother. 70:424-431.

Blair, J. M., V. N. Bavro, V. Ricci, N. Modi, P. Cacciotto, U. Kleinekathöfer, P. Ruggerone, A. V. Vargiu, A. J. Baylay, and H. E. Smith. 2015. AcrB drug-binding pocket substitution confers clinically relevant resistance and altered substrate specificity. Proceedings of the National Academy of Sciences. 112:3511-3516.

Bohnert, J. A., S. Schuster, M. A. Seeger, E. Fahnrich, K. M. Pos, and W. V. Kern. 2008. Site-directed mutagenesis reveals putative substrate binding residues in the *Escherichia coli* RND efflux pump AcrB. J. Bacteriol. 190:8225-8229.

Bywater, R., M. McConville, I. Phillips, and T. Shryock. 2005. The susceptibility to growth-promoting antibiotics of *Enterococcus faecium* isolates from pigs and chickens in Europe. J. Antimicrob. Chemother.56:538-543.

Cha, H. J., R. T. Muller, and K. M. Pos. 2014. Switch-loop flexibility affects transport of large drugs by the promiscuous AcrB multidrug efflux transporter. Antimicrob. Agents Chemother. 58:4767-4772.

Dantzig, A. H., D. P. de Alwis, and M. Burgess. 2003. Considerations in the design and development of transport inhibitors as adjuncts to drug therapy. Adv. Drug Deliv. Rev. 55:133-150.

David, M. Z., and R. S. Daum. 2010. Community-associated methicillin-resistant *Staphylococcus aureus*: epidemiology and clinical consequences of an emerging epidemic. Clin. Microbiol. Rev. 23:616-687.

Davies, J., and D. Davies. 2010. Origins and evolution of antibiotic resistance. Microbiol. Mol. Biol. Rev. 74:417-433.

Delcour, A. H. 2009. Outer membrane permeability and antibiotic resistance. Biochimica Et Biophysica Acta (BBA)-Proteins and Proteomics. 1794:808-816.

Dinh, T., I. T. Paulsen, and M. H. Saier Jr. 1994. A family of extracytoplasmic proteins that allow transport of large molecules across the outer membranes of gram-negative bacteria. J. Bacteriol. 176:3825-3831.

Du, D., H. W. van Veen, and B. F. Luisi. 2015. Assembly and operation of bacterial tripartite multidrug efflux pumps. Trends Microbiol. 23:311-319.

Eicher, T., H. J. Cha, M. A. Seeger, L. Brandstatter, J. El-Delik, J. A. Bohnert, W. V. Kern, F. Verrey, M. G. Grutter, K. Diederichs, and K. M. Pos. 2012. Transport of drugs by the multidrug transporter AcrB involves an access and a deep binding pocket that are separated by a switch-loop. Proc. Natl. Acad. Sci. U. S. A. 109:5687-5692.

Fleming, A. 1942. In-vitro tests of penicillin potency. The Lancet. 239:732-733.

Gerken, H., and R. Misra. 2004. Genetic evidence for functional interactions between TolC and AcrA proteins of a major antibiotic efflux pump of Escherichia coli. Mol. Microbiol. 54:620-631.

Hanahan, D., J. Jessee, and F. R. Bloom. 1991. Plasmid transformation of *Escherichia coli* and other bacteria. Meth. Enzymol. 204:63-113.

Hooper, D. C. 1999. Mechanisms of fluoroquinolone resistance. Drug Resistance Updates. 2:38-55.

Husain, F., M. Bikhchandani, and H. Nikaido. 2011. Vestibules are part of the substrate path in the multidrug efflux transporter AcrB of *Escherichia coli*. J. Bacteriol. 193:5847-5849.

Husain, F., M. Humbard, and R. Misra. 2004. Interaction between the TolC and AcrA proteins of a multidrug efflux system of *Escherichia coli*. J. Bacteriol. 186:8533-8536.

Koronakis, V., A. Sharff, E. Koronakis, B. Luisi, and C. Hughes. 2000. Crystal structure of the bacterial membrane protein TolC central to multidrug efflux and protein export. Nature. 405:914-919.

Kumar, A. and Schweizer, H.P. 2005 Bacterial resistance to antibiotics: active efflux and reduced uptake. Adv Drug Deliv Rev 57: 1486-1513

Lee, A., W. Mao, M. S. Warren, A. Mistry, K. Hoshino, R. Okumura, H. Ishida, and O. Lomovskaya. 2000. Interplay between efflux pumps may provide either additive or multiplicative effects on drug resistance. J. Bacteriol. 182:3142-3150.

Levy, S. B., and B. Marshall. 2004. Antibacterial resistance worldwide: causes, challenges and responses. Nat. Med. 10:S122-S129.

Li, X. Z., P. Plesiat, and H. Nikaido. 2015. The challenge of efflux-mediated antibiotic resistance in Gram-negative bacteria. Clin. Microbiol. Rev. 28:337-418.

Ma, D., D. N. Cook, M. Alberti, N. G. Pon, H. Nikaido, and J. E. Hearst. 1995. Genes acrA and acrB encode a stress-induced efflux system of Escherichia coli. Mol. Microbiol. 16:45-55.

Masi, M., P. Vuong, M. Humbard, K. Malone, and R. Misra. 2007. Initial steps of colicin E1 import across the outer membrane of *Escherichia coli*. J. Bacteriol. 189:2667-2676.

Mehla, K., and J. Ramana. 2016. Structural signature of Ser83Leu and Asp87Asn mutations in DNA gyrase from enterotoxigenic *Escherichia coli* and impact on quinolone resistance. Gene. 576:28-35.

Mikolosko, J., K. Bobyk, H. I. Zgurskaya, and P. Ghosh. 2006. Conformational flexibility in the multidrug efflux system protein AcrA. Structure. 14:577-587.

Misra, R., K. D. Morrison, H. J. Cho, and T. Khuu. 2015. Importance of Real-Time Assays To Distinguish Multidrug Efflux Pump-Inhibiting and Outer Membrane-Destabilizing Activities in *Escherichia coli*. J. Bacteriol.197:2479-2488.

Monroe, S., and R. Polk. 2000. Antimicrobial use and bacterial resistance. Curr. Opin. Microbiol. 3:496-501.

Murakami, S., R. Nakashima, E. Yamashita, T. Matsumoto, and A. Yamaguchi. 2006. Crystal structures of a multidrug transporter reveal a functionally rotating mechanism. Nature. 443:173-179.

Nakashima, R., K. Sakurai, S. Yamasaki, K. Nishino, and A. Yamaguchi. 2011. Structures of the multidrug exporter AcrB reveal a proximal multisite drug-binding pocket. Nature. 480:565-569.

Nikaido, H. 2003. Molecular basis of bacterial outer membrane permeability revisited. Microbiol. Mol. Biol. Rev. 67:593-656.

Nikaido, H., and J. M. Pages. 2012. Broad-specificity efflux pumps and their role in multidrug resistance of Gram-negative bacteria. FEMS Microbiol. Rev. 36:340-363.

Nishino, K., and A. Yamaguchi. 2001. Analysis of a complete library of putative drug transporter genes in *Escherichia coli*. J. Bacteriol. 183:5803-5812.

Okeke, I. N., A. Lamikanra, and R. Edelman. 1999. Socioeconomic and behavioral factors leading to acquired bacterial resistance to antibiotics in developing countries. Emerg. Infect. Dis. 5:18-27.

Paulsen, I. T., J. H. Park, P. S. Choi, and M. H. Saier Jr. 1997. A family of gram-negative bacterial outer membrane factors that function in the export of proteins, carbohydrates, drugs and heavy metals from gram-negative bacteria. FEMS Microbiol. Lett. 156:1-8.

Rosenberg, E. Y., D. Bertenthal, M. L. Nilles, K. P. Bertrand, and H. Nikaido. 2003. Bile salts and fatty acids induce the expression of *Escherichia coli* AcrAB multidrug efflux pump through their interaction with Rob regulatory protein. Mol. Microbiol. 48:1609-1619.

Ruiz, C., and S. B. Levy. 2014. Regulation of acrAB expression by cellular metabolites in *Escherichia coli.* J. Antimicrob. Chemother. 69:390-399.

Seeger, M. A., A. Schiefner, T. Eicher, F. Verrey, K. Diederichs, and K. M. Pos. 2006. Structural asymmetry of AcrB trimer suggests a peristaltic pump mechanism. Science. 313:1295-1298.

Soparkar, K., A. D. Kinana, J. W. Weeks, K. D. Morrison, H. Nikaido, and R. Misra. 2015. Reversal of the Drug Binding Pocket Defects of the AcrB Multidrug Efflux Pump Protein of *Escherichia coli.* J. Bacteriol.197:3255-3264.

Sweeney, L. C., J. Dave, P. A. Chambers, and J. Heritage. 2004. Antibiotic resistance in general dental practice--a cause for concern? J. Antimicrob. Chemother. 53:567-576.

Tamura, N., S. Murakami, Y. Oyama, M. Ishiguro, and A. Yamaguchi. 2005. Direct interaction of multidrug efflux transporter AcrB and outer membrane channel TolC detected via site-directed disulfide cross-linking. Biochemistry (N. Y.). 44:11115-11121.

Tsukagoshi, N., and R. Aono. 2000. Entry into and release of solvents by *Escherichia coli* in an organic-aqueous two-liquid-phase system and substrate specificity of the AcrAB-TolC solvent-extruding pump. J. Bacteriol.182:4803-4810.

Vargiu, A. V., F. Collu, R. Schulz, K. M. Pos, M. Zacharias, U. Kleinekathöfer, and P. Ruggerone. 2011. Effect of the F610A mutation on substrate extrusion in the AcrB transporter: explanation and rationale by molecular dynamics simulations. J. Am. Chem. Soc. 133:10704-10707.

Vargiu, A. V., P. Ruggerone, T. J. Opperman, S. T. Nguyen, and H. Nikaido. 2014. Molecular mechanism of MBX2319 inhibition of *Escherichia coli* AcrB multidrug efflux pump and comparison with other inhibitors. Antimicrob. Agents Chemother. 58:6224-6234.

Wandersman, C., and P. Delepelaire. 1990. TolC, an *Escherichia coli* outer membrane protein required for hemolysin secretion. Proc. Natl. Acad. Sci. U. S. A. 87:4776-4780.

Weeks, J. W., V. N. Bavro, and R. Misra. 2014. Genetic assessment of the role of AcrB β-hairpins in the assembly of the TolC–AcrAB multidrug efflux pump of *Escherichia coli*. Mol. Microbiol. 91:965-975.

Weinstein, R. A. 2001. Controlling antimicrobial resistance in hospitals: infection control and use of antibiotics. Emerg. Infect. Dis. 7:188-192.

World Health Organization. 2014. Antimicrobial resistance: global report on surveillance. World Health Organization.

Zgurskaya, H. I., and H. Nikaido. 2000. Multidrug resistance mechanisms: drug efflux across two membranes. Mol. Microbiol. 37:219-225.